AGU ADVANCING EARTH AND SPACE SCIENCE

Geophysical Research Letters®

Key Points:
- Sand patches can emerge on non-erodible surfaces
- Differing surfaces characteristics control particle behavior
- Field measurements demonstrate the key role of sand transport in bedform initiation

Supporting Information:

Supporting Information may be found in the online version of this article.

Correspondence to:

P. Delorme,
p.m.delorme@hull.ac.uk

Field Evidence for the Initiation of Isolated Aeolian Sand Patches

P. Delorme[1,2] ，**J. M. Nield**[1] ，**G. F. S. Wiggs**[3] ，**M. C. Baddock**[4] ，**N. R. Bristow**[5] ，**J. L. Best**[6] ，**K. T. Christensen**[7] ，and **P. Claudin**[8]

[1]School of Geography and Environmental Science, University of Southampton, Southampton, UK, [2]Now at Energy and Environment Institute, University of Hull, Hull, UK, [3]School of Geography and the Environment, University of Oxford, Oxford, UK, [4]Geography and Environment, Loughborough University, Loughborough, UK, [5]St Anthony Falls Laboratory, Mechanical Engineering, University of Minnesota - Twin Cities, Minneapolis, MN, USA, [6]Departments of Geology, Geography and GIS, and Mechanical Science and Engineering and Ven Te Chow Hydrosystems Laboratory, University of Illinois at Urbana-Champaign, Urbana, IL, USA, [7]Departments of Mechanical, Materials and Aerospace Engineering and Civil, Architectural and Environmental Engineering, Illinois Institute of Technology, Chicago, IL, USA, [8]Physique et Mécanique des Milieux Hétérogènes, CNRS, ESPCI Paris, PSL Research University, Université Paris Cité, Sorbonne Université, Paris, France

Abstract Sand patches are one of the precursors to early stage protodunes and occur widely in both desert and coastal aeolian environments. Here we show field evidence of a mechanism to explain the initiation of sand patches on non-erodible surfaces, such as desert gravels and moist beaches. Changes in sand transport dynamics, directly associated with the height of the saltation layer and variable transport law, observed at the boundary between non-erodible and erodible surfaces lead to sand deposition on the erodible surface. This explains how sand patches can form on surfaces with limited sand availability where linear stability of dune theory does not apply. This new mechanism is supported by field observations that evidence both the change in transport rate over different surfaces and in situ patch formation that leads to modification of transport dynamics at the surface boundary.

Plain Language Summary Sand patches can be observed in various environments such as beaches and gravel plains in deserts. Expected to be precursors of dunes when sediment supply is limited, these bedforms are typically a few centimeters high and present a reverse longitudinal elevation profile, with a sharp upwind edge and a smooth downwind tail. Based on field measurements, we propose a formation mechanism for these patches associated with the sensitive nature of wind-blown sand transport to changing bed conditions: sand saltation is reduced at the transition from a solid to an erodible surface, hence favoring deposition on the patches. This allows us to explain their typical meter-scale length as well as their asymmetric shapes.

1. Introduction

Isolated low-angle sand patches are commonly observed in desert and coastal regions on non-erodible surfaces, such as gravel plains or moist beaches (Figure 1, e.g., Lancaster, 1996; Hesp & Arens, 1997; Nield, 2011). These bedforms are typically several centimeters high, exhibit reverse longitudinal asymmetry compared to mature dunes, and can develop rapidly over several hours. Extensive research has explored the physical dynamics and morphology of mature desert sand dunes (Andreotti et al., 2002a; Bagnold, 1937, 1941; Charru et al., 2013; Courrech du Pont, 2015; Lancaster, 1982; Werner, 1990; Wiggs, 2021). We also have some evidence of the dynamics by which emerging dunes might grow into early stage protodunes and more mature dune forms (Elbelrhiti, 2012; Hage et al., 2018; Kocurek et al., 1992; Montreuil et al., 2020; Nield et al., 2011), where the subtle coupling of topography, wind flow, and sediment transport acts to reinforce their growth (Baddock et al., 2018; Bristow et al., 2022; Delorme et al., 2020; Gadal, Narteau, Ewing, et al., 2020; Lü et al., 2021). However, our knowledge of the processes resulting in, and the relevant time and length scales associated with, the initial deposition of sand on a non-erodible surface remains incomplete and unquantified, although such processes possibly represent a fundamental stage in the origin of aeolian dunes.

There are two clear sets of processes by which aeolian dunes are thought to be established (Courrech du Pont, 2015; Courrech du Pont et al., 2014). The first is associated with the hydrodynamic instability of an erodible granular flat bed with unlimited sand availability (Andreotti et al., 2002a; Charru et al., 2013; Claudin et al., 2013;
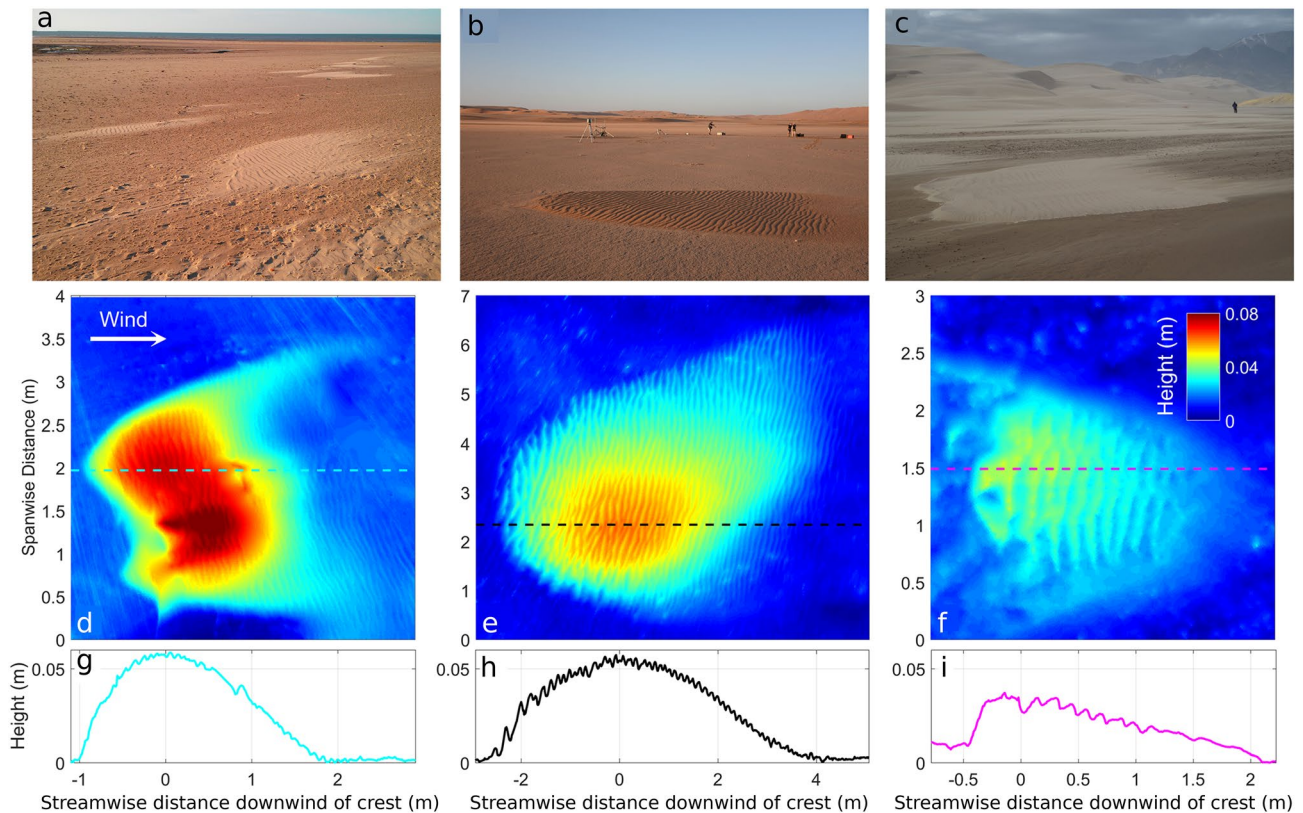
Figure 1. Sand patches formed on different surfaces. Brancaster beach Norfolk, UK (a, d, and g), Helga's dunefield, Namib Desert, Namibia (b, e, and h), and Medano Creek, Great Sand Dunes National Park, Colorado, USA (c, f, and i).

Warren, 1979). This instability results from the combination of the response of wind stress to the modulated topographic profile, and the response of sand transport to the spatial variation in that wind stress (Charru et al., 2013). The former drives the instability where the wind stress maximum is shifted upwind of a dune crest (Claudin et al., 2013; Lü et al., 2021); the latter controls the emerging dune size with a relaxation process over a (saturation) length, L_{sat} (Andreotti et al., 2010; Pähtz et al., 2013; Sauermann et al., 2001; Selmani et al., 2018). The resulting dune pattern consists of straight-crested bedforms growing in amplitude with an orientation controlled by the wind regime (Delorme et al., 2020; Gadal et al., 2019). The second set of processes is associated with the growth of finger-like dunes developing across a non-erodible surface from isolated sand sources (Courrech du Pont et al., 2014; Gadal, Narteau, Du Pont, et al., 2020; Rozier et al., 2019). In this case, the dunes, well separated by interdunes where sand is scarce, present a finger-like shape and grow in length in a direction between those of the dominant winds (Rozier et al., 2019). Experiments in wind tunnels have also highlighted the critical role of boundary conditions in determining saltation dynamics and sand transport rates (e.g., Ho et al., 2012; Kamath et al., 2022) and this offers a potential further means by which dunes may establish. These experiments have provided evidence for the existence of distinctly different transport rates on erodible and non-erodible or moist surfaces (Ho et al., 2011; Neuman & Scott, 1998). Larger sediment fluxes on non-erodible beds have been interpreted as a consequence of a negligible feedback between the mobile grains on the flow. This is in contrast to the wind velocity "focal point" that exists when saltation takes place over an erodible granular bed where the saltating grains comprise a momentum sink on the overlying flow (Bagnold, 1937; Creyssels et al., 2009; Durán et al., 2011; Ho et al., 2014; Ungar & Haff, 1987; Valance et al., 2015).

Here, we propose a new mode for sand patch and protodune initiation associated with the sensitive nature of the transport law in response to changing bed conditions. We find that sand transport rates responding to non-erodible to erodible bed conditions can explain the emergence of isolated, meter-scale sand patches on gravelly interdune areas or moist beaches (Figure 1). Our field data in support of this process, quantitatively capturing the emergence of a sand patch and the change in saltation this produces, allows us to propose a conceptual model for early stage protodune growth from a flat bed.
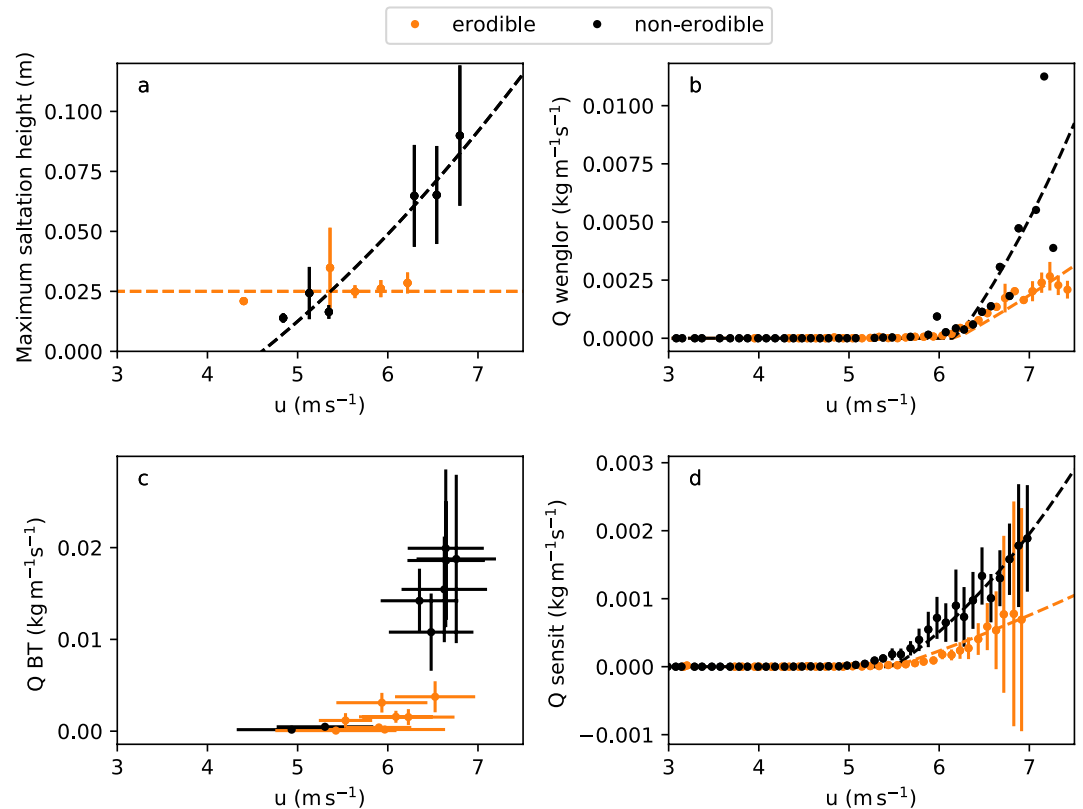
Figure 2. Saltation height (a) and sediment flux (Q) as a function of wind velocity on both surfaces, as measured from Wenglor vertical array (b), Bagnold trap (c), and Sensit counters (d).

2. Methods

Sediment transport measurements were undertaken in the Skeleton Coast National Park, Namibia on sand and gravel surfaces between the 13th and 15th September 2019. Here, wind speed was measured simultaneously on both surfaces using hotwire anemometers (DANTEC 54T35 probes) at a height of 0.085 m and a frequency of 0.1 Hz. Co-located sediment transport was measured via laser particle counters (Wenglor YH03PCT8, following the methods of Barchyn et al. (2014)), Sensit contact particle counters and modified Bagnold sand traps. Saltation height was measured, using a Leica P20 terrestrial laser scanner (TLS) following the methods of Nield and Wiggs (2011), in a 1 m² area immediately upwind of the wind and sand transport instrument arrays, alternating between each of the gravel and sand sites. Additional measurements were undertaken to quantify both saltation height and surface topographic change during the initial formation of a sand patch using Leica P20 and P50 TLS instruments placed downwind of an emerging patch at Great Sand Dunes National Park, Colorado, USA on the 15th April 2019. Details on the data processing methods can be found in Supporting Information S1.

3. Evidence for Differing Sand Transport Processes on Surfaces With Different Erodibility

Our measurements show evidence of different particle behavior over the erodible and non-erodible beds. We find that the saltation height on the erodible surface is invariant with wind velocity whereas it increases with wind velocity on the non-erodible surface, as has been noted by other researchers (Bagnold, 1937, 1941; Creyssels et al., 2009; Ho et al., 2012; Martin & Kok, 2017; Figure 2a). This field measured saltation height behavior then drives a change in sediment transport law on the erodible and non-erodible surface, as confirmed by our three independent measures of sand transport: a vertical array of Wenglor laser counters (Figure 2b), Bagnold type sand traps (Figure 2c), and Sensit piezoelectric counters (Figure 2d).

Figures 2b–2d show that for a given wind velocity, the amount of sand transported over the non-erodible surface is greater than that transported over the erodible surface. According to Bagnold (1937), the velocity of saltating
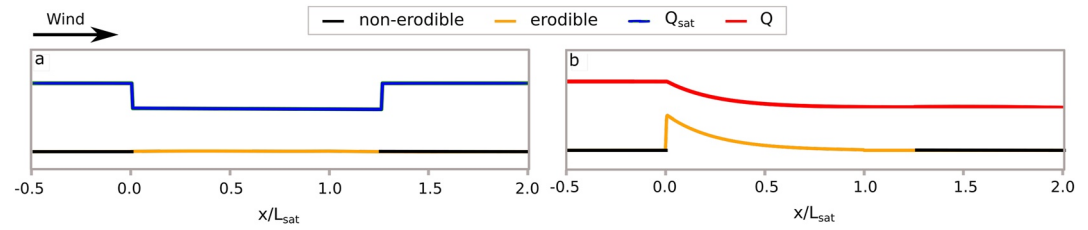
Figure 3. Conceptual model for emergence of a sand patch driven by change in sand transport in the case of limited sand availability surface. (a) Pre-deposition state with the associated potential saturated sand flux (blue line). (b) Post-deposition state, with red line representing the actual sand flux.

grains over the erodible bed is independent of the wind velocity, and consequently the sand flux over an erodible surface scales quadratically with the wind speed (Ungar & Haff, 1987; Werner, 1990, orange dashed lines Figures 2b and 2d). However, over the non-erodible bed, the particle velocity increases with wind velocity, thereby establishing a cubic dependence of sand transport on wind velocity (Ho et al., 2011, black dashed lines Figures 2b and 2d). Two equations can thus be proposed to fit our data sets:

$$Q_{\text{sat}} = p \, Q_{\text{ref}} \frac{u^2 - u_t^2}{u_t^2}, \tag{1}$$

for the erodible surface data sets, and,

$$Q_{\text{sat}} = p \, Q_{\text{ref}} \frac{u^2 - u_t^2}{u_t^2} \frac{u}{u_t}, \tag{2}$$

for the non-erodible surface data sets, with Q_{ref} as the reference flux that is dependent on the sand characteristics, u_t, the threshold velocity, and p, a fitting parameter (see Supporting Information S1 for details on values for each measurement method). Because of this change in transport law, to respect mass balance, the transition from non-erodible to erodible bed should thus generate sand deposition.

4. Bedform Development

4.1. Conceptual Model

Based on our field measurements, we propose a conceptual model to explain the emergence of an isolated sand patch on a flat, non-erodible bed with limited sand availability. We consider a flat, non-erodible surface (represented in black on Figure 3a) adjacent to an erodible zone (in orange). Due to this change in surface characteristics, and according to Equations 1 and 2, a drop in the saturated sand flux at the transition from the non-erodible to erodible surface should occur (blue line on Figure 3a). However, the flux does not adjust instantaneously to its new saturated value, but responds with a characteristic relaxation length, called the saturation length L_{sat}, to reach Q_{sat} (Andreotti et al., 2010; Pähtz et al., 2013; Sauermann et al., 2001; Selmani et al., 2018). The red line represents this decrease in sand flux downwind of the non-erodible/erodible bed boundary (Figure 3b). To respect mass balance, the excess sand transported on the non-erodible surface must deposit at the non-erodible/erodible transition following the decrease in sand flux over L_{sat}, which thereby leads to the formation of a sand deposit (Figure 3b). The rapid decrease in sand flux at the transition from a non-erodible to erodible surface (red line) thus generates a sand patch with an asymmetric shape, possessing a sharp upwind edge with a smooth downwind tail (Figure 3b).

This simple conceptual model assumes a constant wind velocity above threshold, and a sharp transition from a non-erodible to erodible surface. In the next section, we compare qualitatively the topography of an incipient bedform in the field to the idealized patch presented in Figure 3b.

4.2. Field Evidence

Sand transport measurements over a centimeter-high initial sand patch are challenging in the field as the placement of instruments can modify or destroy the emerging bedform by disrupting the windflow. Consequently, we
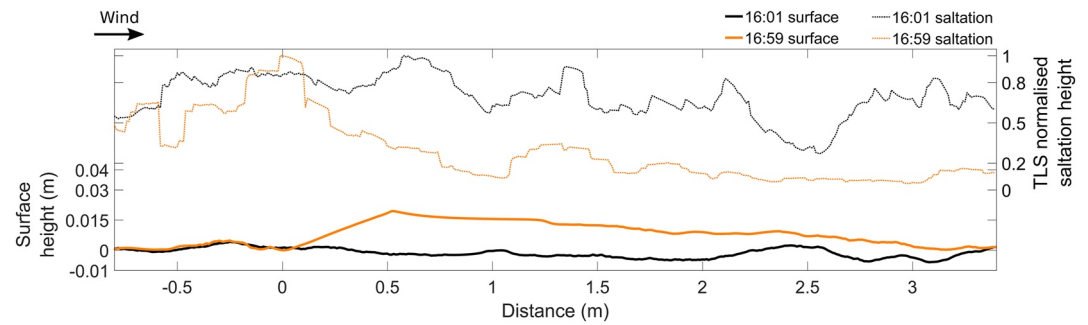
Figure 4. Terrestrial laser scanner measured surface over an hour during the initial development of a sand patch and the corresponding relative saltation height over the same surface. Measurements were undertaken in the Great Sand Dunes National Park. The average wind speed measured at 0.1 m above the surface during the experiment was 6.35 m s^{-1}. Relative saltation height is normalized by the maximum saltation height within each x-minute measurement period (the methods are detailed in Supporting Information S1).

measure concurrently the topography of an emerging sand patch and the saltation layer height with a non-invasive TLS. According to the measurements presented in Figure 2a, we can use the dependence of the saltation layer height upon the wind velocity as a proxy for the appropriate transport law. To confirm that the change in sand flux acts as a driver for sand patch initiation, we measured the topography and saltation layer height pre-(black) and post-(orange) emergence of a sand patch on a sediment availability-limited, non-erodible surface (Figure 4; field site and method are described in Supporting Information S1). Figure 4 shows the height of the saltation layer is constant above the non-erodible surface, whereas it decreases over the developing patch due to its erodible sand surface. When sand particles start to travel over the erodible surface, each grain impact with the bed generates a particle ejection (splash effect), so that this process is consumes energy. Consequently, saltating particles lose energy and experience a lower jump height, causing a decrease in the height of the saltation layer (Bagnold, 1937; Ho et al., 2012, 2014; Valance et al., 2015).

As predicted by our conceptual model (Figure 3), the observed initial sand patch exhibits a reverse asymmetry, with the steepest slope at the upwind edge. Our field measurements (Figure 4) show a rapid decrease in saltation height from the upwind edge of the patch to a distance 1.4 ± 0.3 m downwind of the patch toe. According to our conceptual model, sand deposition occurs over the saturation length. Although the relationship between L_{sat} and the grain diameter is still a matter of debate (Pähtz & Durán, 2017; Pähtz et al., 2013; Selmani et al., 2018), here we follow Andreotti et al. (2010) to estimate L_{sat} as

$$L_{\text{sat}} \approx 2.2 \frac{\rho_s}{\rho} d \qquad (3)$$

At the Great Sand Dunes field site, the grain size is $d = 350 \pm 50$ μm, mass density is $\rho_s = 2{,}650$ kg m^{-3}, and the air density $\rho = 1.2$ kg m^{-3} that yields a saturation length of 1.7 ± 0.25 m, in good agreement with our field measurements. This therefore suggests that the saturation length sets the length of the incipient sand patch.

5. Discussion and Conclusions

Combining field measurements and a simple physically based model, we propose a mechanism to explain the initiation of aeolian sand patches where there is limited sand availability. A change in surface characteristics (erodible/non-erodible or dry/moist) is critical, and leads to a modification of the sand transport dynamics. In agreement with previous studies, we show that the quantity of transported sand, and height of particle saltation, drops when encountering an erodible surface. The corresponding decrease in sand flux generates deposition in order to satisfy mass balance, thus adding sediment to the patch. Moreover, our field measurements demonstrate that the saturation length controls the size of the emerging deposit associated with the spatial relaxation of flux. Besides a change in surface mobility, the second critical parameter controlling sand patch emergence is the incoming sand flux. In our conceptual model, we assume the incoming sand flux equals the saturated sand flux associated with the non-erodible surface. However, the value of incoming flux depends largely on the sand source availability upwind of the initial patch. Without appropriate sand supply, such incipient bedforms

are likely to degrade rapidly (Lancaster, 1996; Nield, 2011). The majority of sand patches develop in interdune areas (Lancaster, 1996) and beaches (Baddock et al., 2018; Hage et al., 2018; Hesp & Arens, 1997; Montreuil et al., 2020; Nield et al., 2011), and in these cases sand sources are provided by the surrounding dry sandy surfaces. However, in the case of a succession or field of patches, if all the excess sand is deposited on the upwind erodible surfaces (as in the case of our conceptual schematics), then sediment supply would be further reduced to downwind patches. This condition likely creates a control on sand feeding of downwind patches and suggests there is a role for temporal wind fluctuations, both in strength and direction, in maintaining a broad field of multiple sand patches. As sand starts to be deposited, the initial bedform will interact with the wind flow and consequently the downwind variation of the sand flux will depend not only on the nature of the substrate (erodible/non-erodible) but also on the underlying and developing topography (Bristow et al., 2022; Claudin et al., 2013; Courrech du Pont, 2015). Consequently, to develop the conceptual arguments presented herein and investigate the conditions under which the aeolian sand patch is most likely to evolve, the present model needs further development to include full coupling between wind, transport and topography. In order to examine propagative solutions in a simplified dune model that accounted for these couplings, Andreotti et al. (2002b) identified flat bedform profiles without slipfaces (patches), but these solutions did not account for the change of transport law when bed conditions varied. However, these results did show the necessity of an incoming flux for these solutions to exist. The present study shows, for the first time, that it is possible to develop a sand patch on a non-erodible surface without any additional perturbation from the topography of the bed, and opens the way for study of the evolution of isolated sand patches toward larger bedforms and fully developed dunes (Bristow et al., 2022; Kocurek et al., 1992).

Data Availability Statement

The data used in this manuscript can be found in the NERC National Geological Data Center: Huab river valley data set (https://doi.org/10.5285/99e4446f-c43a-492d-83c9-e896206649c0, Nield et al., 2022a) and Great Sand Dunes National Park data set (https://doi.org/10.5285/46e9ff95-27ca-4d3b-b587-fc9ce22c5781, Nield et al., 2022b). Supplementary figures and text can be found in Supporting Information S1.

References

Andreotti, B., Claudin, P., & Douady, S. (2002a). Selection of dune shapes and velocities part 1: Dynamics of sand, wind and barchans. *European Physical Journal B: Condensed Matter and Complex Systems*, *28*(3), 321–339. https://doi.org/10.1140/epjb/e2002-00236-4

Andreotti, B., Claudin, P., & Douady, S. (2002b). Selection of dune shapes and velocities part 2: A two-dimensional modelling. *European Physical Journal B: Condensed Matter and Complex Systems*, *28*(3), 341–352. https://doi.org/10.1140/epjb/e2002-00237-3

Andreotti, B., Claudin, P., & Pouliquen, O. (2010). Measurements of the aeolian sand transport saturation length. *Geomorphology*, *123*(3–4), 343–348. https://doi.org/10.1016/j.geomorph.2010.08.002

Baddock, M. C., Nield, J. M., & Wiggs, G. F. S. (2018). Early-stage aeolian protodunes: Bedform development and sand transport dynamics. *Earth Surface Processes and Landforms*, *43*(1), 339–346. https://doi.org/10.1002/esp.4242

Bagnold, R. A. (1937). The transport of sand by wind. *The Geographical Journal*, *89*(5), 409–438. https://doi.org/10.2307/1786411

Bagnold, R. A. (1941). The physics of blown sand and desert dunes.

Barchyn, T. E., Hugenholtz, C. H., Li, B., Neuman, C. M., & Sanderson, R. S. (2014). From particle counts to flux: Wind tunnel testing and calibration of the 'Wenglor' aeolian sediment transport sensor. *Aeolian Research*, *15*, 311–318. https://doi.org/10.1016/j.aeolia.2014.06.009

Bristow, N. R., Best, J., Wiggs, G. F. S., Nield, J. M., Baddock, M. C., Delorme, P., & Christensen, K. T. (2022). Topographic perturbation of turbulent boundary layers by low-angle, early-stage aeolian dunes. *Earth Surface Processes and Landforms*, *47*(6), 1439–1454. https://doi.org/10.1002/esp.5326

Charru, F., Andreotti, B., & Claudin, P. (2013). Sand ripples and dunes. *Annual Review of Fluid Mechanics*, *45*(1), 469–493. https://doi.org/10.1146/annurev-fluid-011212-140806

Claudin, P., Wiggs, G. F. S., & Andreotti, B. (2013). Field evidence for the upwind velocity shift at the crest of low dunes. *Boundary-Layer Meteorology*, *148*(1), 195–206. https://doi.org/10.1007/s10546-013-9804-3

Courrech du Pont, S. (2015). Dune morphodynamics. *Comptes Rendus Physique*, *16*(1), 118–138. https://doi.org/10.1016/j.crhy.2015.02.002

Courrech du Pont, S., Narteau, C., & Gao, X. (2014). Two modes for dune orientation. *Geology*, *42*(9), 743–746. https://doi.org/10.1130/G35657.1

Creyssels, M., Dupont, P., El Moctar, A. O., Valance, A., Cantat, I., Jenkins, J. T., et al. (2009). Saltating particles in a turbulent boundary layer: Experiment and theory. *Journal of Fluid Mechanics*, *625*, 47–74. https://doi.org/10.1017/S0022112008005491

Delorme, P., Wiggs, G. F. S., Baddock, M. C., Claudin, P., Nield, J. M., & Valdez, A. (2020). Dune initiation in a bimodal wind regime. *Journal of Geophysical Research: Earth Surface*, *125*(11), e2020JF005757. https://doi.org/10.1029/2020JF005757

Durán, O., Claudin, P., & Andreotti, B. (2011). On aeolian transport: Grain-scale interactions, dynamical mechanisms and scaling laws. *Aeolian Research*, *3*(3), 243–270. https://doi.org/10.1016/j.aeolia.2011.07.006

Elbelrhiti, H. (2012). Initiation and early development of Barchan dunes: A case study of the Moroccan Atlantic Sahara desert. *Geomorphology*, *138*(1), 181–188. https://doi.org/10.1016/j.geomorph.2011.08.033

Gadal, C., Narteau, C., Du Pont, S. C., Rozier, O., & Claudin, P. (2019). Incipient bedforms in a bidirectional wind regime. *Journal of Fluid Mechanics*, *862*, 490–516. https://doi.org/10.1017/jfm.2018.978

Gadal, C., Narteau, C., Du Pont, S. C., Rozier, O., & Claudin, P. (2020). Periodicity in fields of elongating dunes. *Geology*, *48*(4), 343–347. https://doi.org/10.1130/G46987.1

Gadal, C., Narteau, C., Ewing, R., Gunn, A., Jerolmack, D., Andreotti, B., & Claudin, P. (2020). Spatial and temporal development of incipient dunes. *Geophysical Research Letters*, *47*(16), e2020GL088919. https://doi.org/10.1029/2020GL088919

Hage, P., Ruessink, B., & Donker, J. (2018). Determining sand strip characteristics using Argus video monitoring. *Aeolian Research*, *33*, 1–11. https://doi.org/10.1016/j.aeolia.2018.03.007

Hesp, P. A., & Arens, S. M. (1997). Crescentic dunes at Schiermonnikoog, The Netherlands. *Earth Surface Processes and Landforms: The Journal of the British Geomorphological Group*, *22*(8), 785–788. https://doi.org/10.1002/(SICI)1096-9837(199708)22:8(785::AID-ESP813)3.0.CO;2-F

Ho, T. D., Dupont, P., El Moctar, A. O., & Valance, A. (2012). Particle velocity distribution in saltation transport. *Physical Review E*, *85*(5), 052301. https://doi.org/10.1103/PhysRevE.85.052301

Ho, T. D., Valance, A., Dupont, P., & El Moctar, A. O. (2011). Scaling laws in aeolian sand transport. *Physical Review Letters*, *106*(9), 094501. https://doi.org/10.1103/PhysRevLett.106.094501

Ho, T. D., Valance, A., Dupont, P., & El Moctar, A. O. (2014). Aeolian sand transport: Length and height distributions of saltation trajectories. *Aeolian Research*, *12*, 65–74. https://doi.org/10.1016/j.aeolia.2013.11.004

Kamath, S., Shao, Y., & Parteli, E. J. R. (2022). Scaling laws in aeolian sand transport under low sand availability. *Geophysical Research Letters*, *49*(11), e2022GL097767. https://doi.org/10.1029/2022GL097767

Kocurek, G., Townsley, M., Yeh, E., Havholm, K. G., & Sweet, M. L. (1992). Dune and dune-field development on Padre Island, Texas, with implications for interdune deposition and water-table-controlled accumulation. *Journal of Sedimentary Research*, *62*(4), 622–635. https://doi.org/10.1306/D4267974-2B26-11D7-8648000102C1865D

Lancaster, N. (1982). Dunes on the skeleton coast, Namibia (south west Africa): Geomorphology and grain size relationships. *Earth Surface Processes and Landforms*, *7*(6), 575–587. https://doi.org/10.1002/esp.3290070606

Lancaster, N. (1996). Field studies of sand patch initiation processes on the northern margin of the Namib sand sea. *Earth Surface Processes and Landforms*, *21*(10), 947–954. https://doi.org/10.1002/(SICI)1096-9837(199610)21:10(947::AID-ESP634)3.0.CO;2-7

Lü, P., Narteau, C., Dong, Z., Claudin, P., Rodriguez, S., An, Z., et al. (2021). Direct validation of dune instability theory. *Proceedings of the National Academy of Sciences of the United States of America*, *118*(17), e2024105118. https://doi.org/10.1073/pnas.2024105118

Martin, R. L., & Kok, J. F. (2017). Wind-invariant saltation heights imply linear scaling of aeolian saltation flux with shear stress. *Science Advances*, *3*(6), e1602569. https://doi.org/10.1126/sciadv.1602569

Montreuil, A.-L., Chen, M., Brand, E., De Wulf, A., De Sloover, L., Dan, S., & Verwaest, T. (2020). Early-stage aeolian dune development and dynamics on the upper-beach. *Journal of Coastal Research*, *95*(SI), 336–340. https://doi.org/10.2112/SI95-065.1

Neuman, C. M., & Scott, M. M. (1998). A wind tunnel study of the influence of pore water on aeolian sediment transport. *Journal of Arid Environments*, *39*(3), 403–419. https://doi.org/10.1006/jare.1997.0371

Nield, J. M. (2011). Surface moisture- induced feedback in aeolian environments. *Geology*, *39*(10), 915–918. https://doi.org/10.1130/G32151.1

Nield, J. M., & Wiggs, G. F. S. (2011). The application of terrestrial laser scanning to aeolian saltation cloud measurement and its response to changing surface moisture. *Earth Surface Processes and Landforms*, *36*(2), 273–278. https://doi.org/10.1002/esp.2102

Nield, J. M., Wiggs, G. F. S., Baddock, M. C., & Delorme, P. (2022a). Surface and meteorological data at Huab river valley, skeleton coast national park, Namibia in September 2019 [Dataset]. NERC EDS National Geoscience Data Centre. https://doi.org/10.5285/99e4446f-c43a-492d-83c9-e896206649c0

Nield, J. M., Wiggs, G. F. S., Baddock, M. C., & Delorme, P. (2022b). Surface and meteorological data at medano creek, great sand dunes national park, Colorado, USA on 15th April 2019 [Dataset]. NERC EDS National Geoscience Data Centre. https://doi.org/10.5285/46e9ff95-27ca-4d3b-b587-fc9ce22c5781

Nield, J. M., Wiggs, G. F. S., & Squirrell, R. S. (2011). Aeolian sand strip mobility and protodune development on a drying beach: Examining surface moisture and surface roughness patterns measured by terrestrial laser scanning. *Earth Surface Processes and Landforms*, *36*(4), 513–522. https://doi.org/10.1002/esp.2071

Pähtz, T., & Durán, O. (2017). Fluid forces or impacts: What governs the entrainment of soil particles in sediment transport mediated by a Newtonian fluid? *Physical Review Fluids*, *2*(7), 074303. https://doi.org/10.1103/PhysRevFluids.2.074303

Pähtz, T., Kok, J. F., Parteli, E. J. R., & Herrmann, H. J. (2013). Flux saturation length of sediment transport. *Physical Review Letters*, *111*(21), 218002. https://doi.org/10.1103/PhysRevLett.111.218002

Rozier, O., Narteau, C., Gadal, C., Claudin, P., & Courrech du Pont, S. (2019). Elongation and stability of a linear dune. *Geophysical Research Letters*, *46*(24), 14521–14530. https://doi.org/10.1029/2019GL085147

Sauermann, G., Kroy, K., & Herrmann, H. J. (2001). Continuum saltation model for sand dunes. *Physical Review E*, *64*(3), 031305. https://doi.org/10.1103/PhysRevE.64.031305

Selmani, H., Valance, A., Ould El Moctar, A., Dupont, P., & Zegadi, R. (2018). Aeolian sand transport in out-of-equilibrium regimes. *Geophysical Research Letters*, *45*(4), 1838–1844. https://doi.org/10.1002/2017GL076937

Ungar, J. E., & Haff, P. K. (1987). Steady state saltation in air. *Sedimentology*, *34*(2), 289–299. https://doi.org/10.1111/j.1365-3091.1987.tb00778.x

Valance, A., Rasmussen, K. R., El Moctar, A. O., & Dupont, P. (2015). The physics of aeolian sand transport. *Comptes Rendus Physique*, *16*(1), 105–117. https://doi.org/10.1016/j.crhy.2015.01.006

Warren, A. (1979). Aeolian processes. *Process in Geomorphology*, *325*, S1.

Werner, B. T. (1990). A steady-state model of wind-blown sand transport. *The Journal of Geology*, *98*(1), 1–17. https://doi.org/10.1086/629371

Wiggs, G. (2021). *7.17 dune morphology and dynamics. Treatise on Geomorphology* (2nd ed.). Academic Press. https://doi.org/10.1016/B978-0-12-818234-5.00073-